Nanoscale

COMMUNICATION

View Article Online
View Journal | View Issue

Cite this: *Nanoscale*, 2019, **11**, 13227

Received 26th March 2019,
Accepted 1st July 2019

DOI: 10.1039/c9nr02617g

rsc.li/nanoscale

Electronic shells of a tubular Au_{26} cluster: a cage–cage superatomic molecule based on spherical aromaticity†

Qiman Liu,‡[a] Chang Xu,‡[a] Xia Wu*[b] and Longjiu Cheng *[a,c]

Gold clusters, which display a variety of unusual geometric structures due to their strong relativistic effects, have attracted much attention. Among them, Au_{26} has a high-symmetry tubular structure (D_{6d}) with a large HOMO–LUMO energy gap, but its electronic stability still remains unclear. In this paper, the electronic nature of the Au_{26} cluster is investigated using the density functional theory method. Depending on the super valence bond model, the tubular Au_{26} cluster with 26 valence electrons could be viewed as a superatomic molecule composed of two open cages based on spherical aromaticity, and its molecule-like electronic shell closure is achieved *via* a super triple bond (σ, 2π) between the two cages. Based on this new cage–cage superatomic structural model, a series of similar tubular clusters are predicted from the Au_{26} skeleton. The two capped Au atoms are replaced by Cu, Ag and In atoms, respectively, to form tubular D_{6d} $Au_{24}Cu_2$ and $Au_{24}Ag_2$ (26e) and $Au_{24}In_2$ (30e) clusters, where the super triple bonds also exist. Moreover, tubular D_{5d} $Au_{20}In_2$ (26e) is obtained by replacing hexatomic Au_6 rings in the bulk of $Au_{24}In_2$ with pentagonal Au_5 rings. Chemical bonding analysis reveals that there is a super quintuple bond (σ, 2π, 2δ) between two open ($Au_{10}In$) cages, in accordance with the 26e $Li_{20}Mg_3$ superatomic molecule composed of two icosahedral superatoms. Our study proposes the new cage–cage structural model of superatomic molecules based on spherical aromaticity, which extends the range of the super valence bonding pattern and gives inferences for further study of superatomic clusters.

Introduction

Nanoscale gold clusters possess unique physical and chemical properties and are widely used as catalysts and electronic devices and in the biochemical industry.[1–4] These fascinating properties arise from the strong relativistic effects of gold, which result in significant s–d hybridization relative to that of other coin metals[5–8] and lead to unusual geometric structures of gold clusters.[9–13] The structures of small-sized gold clusters have been well established which display remarkable planar (2D) structures up to n = 13,[14–17] while even more exotic structures are possible with medium-sized clusters, such as the golden pyramid[18,19] and hollow golden cages.[20–24]

The spherical cage is a popular structural pattern among the gold clusters, such as Au_{32}.[25,26] It is one of the classical gold clusters, which exhibits an icosahedral (I_h) hollow cage structure with the energy gap of 2.49 eV between the highest occupied molecular orbital and the lowest unoccupied molecular orbital (HOMO–LUMO). The geometric shell closure and a remarkably large HOMO–LUMO gap indicate its superatomic character.[27] Moreover, there are 32 valence electrons in the superatomic orbitals of this cluster, which satisfy the $2(N+1)^2$ rule of spherical aromaticity (see Fig. S1 in the ESI†). Similar golden cages, such as Au_{50} and Au_{72}, also follow the same rule.[28–30] For these superatoms with hollow cage structures, the valence electrons are delocalized on the surface of the cages which could be viewed as a nodal plane,[31–34] and follow the aromatic $2(N+1)^2$ rule for the electronic shell closure, in which the magic electronic numbers are 2, 8, 18, 32..., with different values of N. This is different from the classical Jellium model[35–38] and three-dimensional aromaticity,[39–45] in which the valence electrons are delocalized in the whole cluster.

Among the diversity of gold clusters, Au_{26} is one of the special species, for which there is a long lasting debate regarding its geometric structure. Dong *et al.*[46] point out that a high-symmetry D_{6d} tubular structure is due to the possible ground state of the cluster which could be viewed as the combination

[a]*Department of Chemistry, Anhui University, Hefei, Anhui 230601, P. R. China. E-mail: clj@ustc.edu*
[b]*School of Chemistry and Chemical Engineering, Anqing Normal University, Anqing, 246011, P. R. China. E-mail: xiawu@aqnu.edu.cn*
[c]*Anhui Province Key Laboratory of Chemistry for Inorganic/Organic Hybrid Functionalized Materials, Hefei, Anhui, 230601, P. R. China*

†Electronic supplementary information (ESI) available: The partial canonical molecular orbitals of Au_{32} and $Au_{20}In_2$ clusters and the AdNDP localized natural bonding orbitals of the valence shells of $Au_{24}Ag_2$, $Au_{24}Cu_2$ and $Au_{20}Ga_2$ clusters. See DOI: 10.1039/c9nr02617g

‡These two authors contributed equally to this work.

of four Au_6 rings with two more Au atoms in the center of the two side faces, while another theoretical report indicates that Au_{26} adopts an fcc-like structure.[47] Later, Wang and co-workers carried out extensive structure predictions and demonstrated that the Au_{26} cluster is a fluxional system with a large number of metastable isomers within a narrow energy window.[48] More recently, Joshi *et al.*[49] reveal that the tubular structure is most thermally stable among the four conformations (three compact or core–shell structures and a high symmetry tubular structure).

The tubular Au_{26} cluster attracts much interest due to its peculiar geometric structure which could be the embryo of an Au nanotube.[50] The closed-shell geometry and large HOMO–LUMO energy gap indicate that this cluster would have a molecule-like electronic shell closure. However, the electronic character of this cluster still remains unclear. It cannot be described by the superatom model of spherical aromaticity due to its non-spherical structure. Recently, the super valence bond (SVB) model was proposed by Cheng and Yang to explain the electronic stability of non-spherical metallic clusters.[51] In the SVB model, a prolate cluster could be divided into two spherical blocks sharing the atomic nucleus at the border, of which each block is viewed as a superatom following the electronic shells in the Jellium model, and molecule-like electronic shell-closure is achieved by the sharing of electron pairs between the two superatoms. The SVB model has been successfully used in explaining the stability of the non-spherical superatomic molecules.[52–58] In addition to the super covalent bonds between the superatoms, another kind of superatomic bond – the super hybrid bond – is revealed in gold clusters,[59–62] such as the Au_{42} cluster composed of hybrid SP^2 Au_6 superatomic units.[60] A recent study reveals an 8e $[Au_{12}(SR)_6]^{2-}$ cluster with a hybrid SP^3 core, which exhibits the special bonding and optical properties.[62]

In this paper, we try to explain the electronic structure of the tubular Au_{26} through the SVB model. Due to the prolate structure of the typical superatomic molecules, it is inferred that the Au_{26} cluster could be divided into two spherical open cages which form the electronic shell-closure through super valence bonds. These separated cages should be described as superatoms based on the spherical aromaticity, which extends the range of the spherical superatom–superatom structural pattern based on the Jellium model used in former SVB studies. Chemical bonding analyses are discussed in the following section to verify our inference, and similar tubular superatomic molecules are designed based on this new bonding model.

Computational method and details

Geometry optimizations and subsequent calculations are performed using the non-empirical hybrid GGA functional PBE0[63] with the def2-TZVP basis set[64] by the density functional theory method. The vibrational frequencies are checked to ensure that the structures are true local minima at the same theoretical level. Chemical bonding analyses are carried out using the adaptive natural density partitioning (AdNDP) method to reveal the molecular orbitals (MOs) of the clusters,[65,66] which is a generalized natural bonding orbital (NBO) search method to discuss the localized and delocalized multicenter bonds (coded as *nc*-2e, that is, an *n*-center two-electron bond). All calculations are performed using the Gaussian 09 package,[67] and molecular visualization is performed using MOLEKEL 5.4 software.[68]

Results and discussion

Electronic character of the Au_{26} superatomic molecule

The optimized tubular $D_{6d}Au_{26}$ cluster[46] with the HOMO–LUMO energy gap (E_{HL}) of 1.34 eV is shown in Fig. 1a. The large gap indicates high electronic stability. However, gold with 26valence electrons dissatisfies the $2(N + 1)^2$ rule for spherical aromaticity. We find that the tubular structure can be divided into two spherical cages, where each cage has 13 valence electrons. As the magic numbers are 2, 8, 18, 32... for the superatomic cage cluster with spherical aromaticity, could this Au_{13} cage be viewed as an open shell superatom? In order to verify our inference, the closed shell $Au_{12}In_2$ cluster with 18 valence electrons is built from the Au_{13} open cage by removing its central Au atom in the side face and capping the rest of the Au_{12} double ring with two In atoms. The optimized geometric structure of the $Au_{12}In_2$ cluster is plotted in Fig. 1b, and the vibration frequency is checked to verify that it is a true local minimum on the potential energy surface. This cluster maintains the D_{6d} symmetry and has a fairly large HOMO–LUMO energy gap of 2.76 eV, suggesting its superatomic character. Moreover, the AdNDP results reveal that the 18 valence electrons of the $Au_{12}In_2$ cluster fill nine MOs, which could be viewed as the super SP^3D^5 orbitals from their shapes (Fig. 1b). These valence electrons distributed on the surface of the cage follow the $2(N + 1)^2$ rule of spherical aromaticity, which indicates its electronic closed shell structure and confirms the superatomic character of the spherical cage. Therefore, Au_{13}

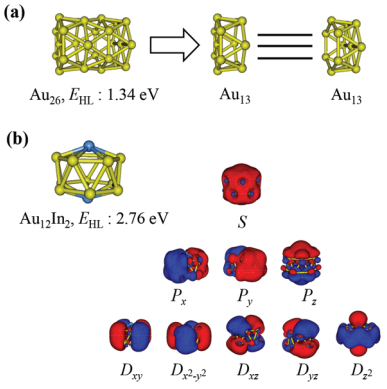

Fig. 1 (a) Di-superatomic model for the tubular Au_{26} cluster. (b) Structure and MO diagrams of the $Au_{12}In_2$ cluster.

with the same skeleton also could be viewed as a superatomic cage, but it exhibits both geometric and electronic open shell characteristics.

Based on the superatomic character of Au_{13}, it could be inferred that the Au_{26} cluster is a superatomic molecule composed of two Au_{13} cages which achieve the electronic shell closure through the super valence bonds. To verify this inference, the canonical molecular orbitals (MOs) of the Au_{26} cluster are investigated as shown in Fig. 2a, and further AdNDP analysis shown in Fig. 2b gives a more clear description of the superatomic molecular framework of Au_{26}. The AdNDP results reveal that there are five 13c–2e super lone pairs (LPs) in each Au_{13} cage (S, P_x, P_y, D_{xy}, and $D_{x^2-y^2}$) which correspond to five bonding orbitals (σ_s, $2\pi_{px,\ y}$, $2\delta_{dxy,\ x2-y2}$) and five antibonding orbitals (σ^*_s, $2\pi^*_{px,\ y}$, $2\delta^*_{dxy,\ x2-y2}$) in MO diagrams. The remaining three occupied MOs (σ, 2π) could be viewed as one 26c–2e super σ-bond composed of two P_z orbitals and two double-degenerate π-bonds formed by D_{xz}–D_{xz} and D_{yz}–D_{yz} interactions. Therefore, the two superatomic cages form a super triple bonding system in this 26e Au_{26} cluster, but its electronic structure is different from another typical 26e superatomic molecule composed of two superatomic spheres – the double-icosahedral $Li_{20}Mg_3$ cluster,[58] in which there is a super quintuple bond (σ, 2π, 2δ) between the two icosahedra.

Prediction of new cage–cage superatomic molecules

The new cage–cage structural model of superatomic molecules is revealed from the electronic nature of the Au_{26} cluster, based on the rule of spherical aromaticity. Then a series of similar cage–cage superatomic molecules are designed from the skeleton of Au_{26}.

To obtain superatomic molecules with different valence electrons, the two capped Au atoms in the center of the top and bottom layers of Au_{26} are replaced by other metal atoms. The isoelectronic $Au_{24}Cu_2$ and $Au_{24}Ag_2$ clusters (Fig. S2†) are built by replacing the capped Au atoms with Cu and Ag atoms, respectively. After relaxation, these two clusters maintain the D_{6d} symmetries with large HOMO–LUMO energy gaps. As they are isoelectronic clusters of Au_{26}, super triple bonds also exist in these clusters as shown in Fig. S2,† which are confirmed by the AdNDP analyses.

The 30e superatomic molecule was investigated in a former study on the $Li_{18}Mg_3Al_2$ cluster[58] composed of two superatomic spheres, which is another kind of a typical superatomic cluster. Therefore, we also design the 30e cage–cage superatomic molecule in this section by replacing the capped Au atoms with In atoms. This $Au_{24}In_2$ cluster maintains the D_{6d} symmetry with the HOMO–LUMO gap of 2.50 eV after relaxation, as shown in Fig. 3. AdNDP calculations reveal that there is a super triple bonding system in the $Au_{24}In_2$ superatomic molecule. Compared with Au_{26}, this cluster has two more super P_z LPs, and its super σ bond is supposed to be formed by D_{z^2}–D_{z^2} interactions in the two superatomic units, which is different from the Au_{26} cluster. Due to the long and thin structure of $Au_{24}In_2$, the P_z superatomic orbitals in the ($Au_{12}In$) cages could not interact with each other and exist as lone electronic pairs. Therefore, in this 30e cage–cage superatomic $Au_{24}In_2$ molecule, each superatomic cage achieves the 18e electronic closed shell structure through the super triple bonding framework with a fairly large HOMO–LUMO gap. It is also different from the $Li_{18}Mg_3Al_2$ cluster with the double-icosahedral structure based on the Jellium model, in which the molecule-like electronic shell closure is achieved *via* quintuple super bonding (σ, 2π, 2δ) between the two icosahedra.

Besides the Au_6 rings, pentagonal Au_5 rings are also possible structural units of nanotubes. Therefore, the $Au_{20}In_2$ superatomic molecule is designed by replacing the hexatomic

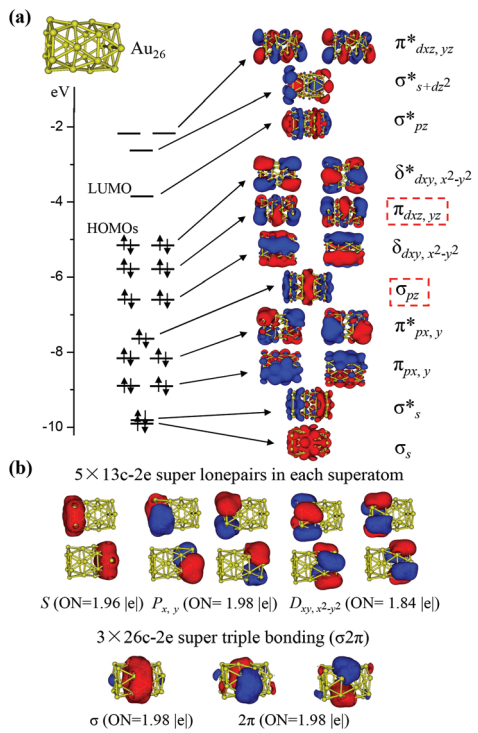

Fig. 2 (a) Structure and the MO diagrams of the Au_{26} cluster. (b) AdNDP localized natural bonding orbitals of the Au_{26} cluster.

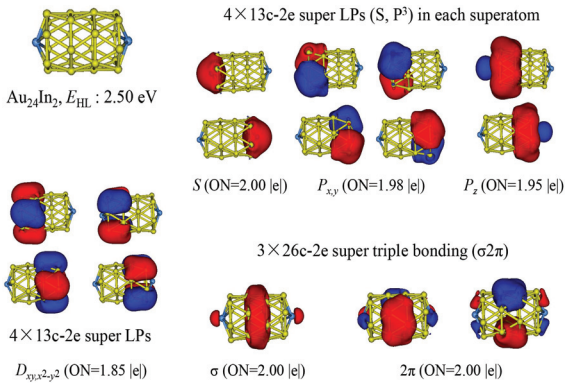

Fig. 3 Structure and AdNDP localized natural bonding orbitals of the $Au_{24}In_2$ cluster.

Au_6 ring in the bulk of the $Au_{24}In_2$ cluster with the pentagonal Au_5 ring, in order to change the structural framework of the cage–cage superatomic molecule. The optimized $Au_{20}In_2$ cluster maintains good stability with the D_{5d} symmetry, as shown in Fig. 4. Unbiased global searches are performed by using the genetic algorithm (GA-DFT) implemented by our group.[69,70] The global minimum and low-energy isomers of the $Au_{20}In_2$ cluster are displayed in Fig. S3.† We found that isomers N.1 and tubular D_{5d} N.2 are nearly degenerate with N.1 being 0.02 eV more stable. Moreover, the tubular $Au_{20}In_2$ cluster is verified to have good thermal stability by *ab initio* molecular dynamics (AIMD) simulations.[71–73] Details for the AIMD simulations are shown in Fig. S4.† Further MOs (Fig. S5†) and AdNDP analyses reveal that this cluster with 26 valence electrons contains four 11c-2e super (SP^3) LPs in each cage ($Au_{10}In$) and a 22c-2e super quintuple bond (σ, 2π, 2δ) between cages, which resembles the $Li_{20}Mg_3$ superatomic molecule in the bonding framework. Similarly, the 26e $Au_{20}Ga_2$ cluster with a pentagonal tubular structure is also studied to confirm the reliability of this structural pattern, and chemical bonding analysis reveals that its bonding framework is the same as the $Au_{20}In_2$ cluster (Fig. S6†).

To further confirm the existence of super bonding, bond energies (E_b) and Mayer bond orders[74] (MBO) are also calculated using different methods and listed in Table 1. The values of E_b and MBO increase from the super triple bond to the super quintuple bond, which are in accordance with their bonding characteristics. It is worth noting that the E_b values are strongly influenced by the dispersion correction D3.[75] Moreover, due to the significant aurophilic interaction in the Au clusters, the bond order between the two cages is relatively large.

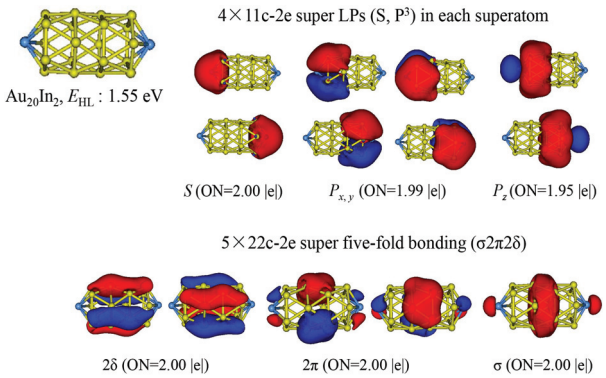

Fig. 4 Structure and AdNDP localized natural bonding orbitals of the $Au_{20}In_2$ cluster.

Table 1 The bond energies (E_b) and Mayer bond orders (MBO) between the two superatomic units for Au_{26} and $Au_{20}In_2$ clusters calculated using different methods

E_b (eV)	PBE0	PBE	PBE-D3	MBO
Au_{13}–Au_{13}	8.82	8.72	9.96	5.9
$Au_{10}In$–$Au_{10}In$	10.21	9.88	11.05	6.0

Conclusions

In summary, the new cage–cage superatomic structural pattern is revealed from the electronic nature of the tubular Au_{26} cluster based on the SVB model. Chemical bonding analysis reveals that this cluster is a superatomic molecule composed of two Au_{13} superatomic open cages with spherical aromaticity, and its molecule-like electronic shell closure is achieved *via* super triple bonds (σ, 2π) between the two cages. Based on this new superatomic structural pattern, a series of cage–cage superatomic molecules are predicted from the skeleton of Au_{26}. 26e $Au_{24}Cu_2$, $Au_{24}Ag_2$ and 30e $Au_{24}In_2$ are designed by replacing the capped Au atoms by Cu, Ag and In atoms, where the super triple bonds also exist. Moreover, the hexatomic Au_6 rings in $Au_{24}In_2$ are replaced by pentagonal Au_5 rings to form the 26e $Au_{20}In_2$ cluster, in which there is a super quintuple bond (σ, 2π, 2δ) between the two ($Au_{10}In$) cages, similar to the 26e $Li_{20}Mg_3$ superatomic molecule composed of two icosahedral superatoms.

Our study reveals the electronic nature of the tubular Au_{26} cluster, which extends the community of super valence bonding patterns and gives inferences for the further investigation of superatomic clusters.

Conflicts of interest

There are no conflicts to declare.

Acknowledgements

This work is financed by the National Natural Science Foundation of China (21873001) and by the Foundation of Distinguished Young Scientists of Anhui Province. The calculations were carried out at the High-Performance Computing Center of Anhui University.

Notes and references

1 H. Hakkinen, *Chem. Soc. Rev.*, 2008, **37**, 1847–1859.
2 G. J. Hutchings, M. Brust and H. Schmidbaur, *Chem. Soc. Rev.*, 2008, **37**, 1759–1765.
3 M. S. Chen and D. W. Goodman, *Science*, 2004, **306**, 252–255.
4 G. Li and R. Jin, *Acc. Chem. Res.*, 2013, **46**, 1749–1758.
5 P. Pyykkö, *Chem. Rev.*, 1988, **88**, 563.
6 H. Häkkinen, M. Moseler and U. Landman, *Phys. Rev. Lett.*, 2002, **89**, 033401.
7 S. Gilb, P. Weis, F. Furche, R. Ahlrichs and M. M. Kappes, *J. Chem. Phys.*, 2002, **116**, 4094–4101.
8 R. Jin, *Nanoscale*, 2010, **2**, 343–362.

9 S. Pande, W. Huang, N. Shao, L. Wang, N. Khetrapal, W. Mei, T. Jian, L. S. Wang and X. C. Zeng, *ACS Nano*, 2016, **10**, 10013–10022.
10 L. Ferrighi, B. Hammer and G. K. H. Madsen, *J. Am. Chem. Soc.*, 2009, **131**, 10605–10609.
11 Y. Gao, S. Bulusu and X. C. Zeng, *J. Am. Chem. Soc.*, 2005, **127**, 15680–15681.
12 N. Shao, W. Huang, W.-N. Mei, L. S. Wang, Q. Wu and X. C. Zeng, *J. Phys. Chem. C*, 2014, **118**, 6887–6892.
13 Y. Pei and X. C. Zeng, *Nanoscale*, 2012, **4**, 4054–4072.
14 J. Wang, G. Wang and J. Zhao, *Phys. Rev. B: Condens. Matter Mater. Phys.*, 2002, **66**, 035418.
15 J. Zhao, J. Yang and J. G. Hou, *Phys. Rev. B: Condens. Matter Mater. Phys.*, 2003, **67**, 085404.
16 R. M. Olson, S. Varganov, M. S. Gordon, H. Metiu, S. Chretien, P. Piecuch, K. Kowalski, S. A. Kucharski and M. Musial, *J. Am. Chem. Soc.*, 2005, **127**, 1049–1052.
17 H. Häkkinen and U. Landman, *Phys. Rev. B: Condens. Matter Mater. Phys.*, 2000, **62**, R2287–R2290.
18 J. Li, X. Li, H. J. Zhai and L. S. Wang, *Science*, 2003, **299**, 864–867.
19 P. Gruene, D. M. Rayner, B. Redlich, A. F. G. van der Meer, J. T. Lyon, G. Meijer and A. Fielicke, *Science*, 2008, **321**, 674–676.
20 E. M. Fernández, J. M. Soler and L. C. Balbás, *Phys. Rev. B: Condens. Matter Mater. Phys.*, 2006, **73**, 235433.
21 X. Gu, M. Ji, S. H. Wei and X. G. Gong, *Phys. Rev. B: Condens. Matter Mater. Phys.*, 2004, **70**, 205401.
22 S. Bulusu and X. C. Zeng, *J. Chem. Phys.*, 2006, **125**, 154303.
23 Y. Gao and X. C. Zeng, *J. Am. Chem. Soc.*, 2005, **127**, 3698–3699.
24 N. S. Khetrapal, S. S. Bulusu and X. C. Zeng, *J. Phys. Chem. A*, 2017, **121**, 2466–2474.
25 M. P. Johansson, D. Sundholm and J. Vaara, *Angew. Chem., Int. Ed.*, 2004, **43**, 2678–2681.
26 M. Ji, X. Gu, X. Li, X. Gong, J. Li and L. S. Wang, *Angew. Chem., Int. Ed.*, 2005, **44**, 7119–7123.
27 M. P. Johansson, J. Vaara and D. Sundholm, *J. Phys. Chem. C*, 2008, **112**, 19311–19315.
28 D. Tian, J. Zhao, B. Wang and R. B. King, *J. Phys. Chem. A*, 2007, **111**, 411–414.
29 A. J. Karttunen, M. Linnolahti, T. A. Pakkanen and P. Pyykko, *Chem. Commun.*, 2008, 465–467.
30 L. Zhi-Ru, W. Fang-Fang, W. Di, L. Ying, C. Wei, S. Xiao-Ying, G. F. Long and A. Yuriko, *J. Comput. Chem.*, 2006, **27**, 986–993.
31 M. Bühl and A. Hirsch, *Chem. Rev.*, 2001, **101**, 1153–1184.
32 A. Hirsch, Z. Chen and H. Jiao, *Angew. Chem., Int. Ed.*, 2001, **113**, 2916–2920.
33 J. Wang, J. Jellinek, J. Zhao, Z. Chen, R. B. King and P. von Ragué Schleyer, *J. Phys. Chem. A*, 2005, **109**, 9265–9269.
34 J. Poater and M. Solà, *Chem. Commun.*, 2011, **47**, 11647–11649.
35 W. D. Knight, K. Clemenger, W. A. de Heer, W. A. Saunders, M. Y. Chou and M. L. Cohen, *Phys. Rev. Lett.*, 1984, **52**, 2141–2143.
36 M. Brack, *Rev. Mod. Phys.*, 1993, **65**, 677–732.
37 A. C. Reber, S. N. Khanna and A. W. Castleman, *J. Am. Chem. Soc.*, 2007, **129**, 10189–10194.
38 D. E. Bergeron, P. J. Roach, A. W. Castleman, N. O. Jones and S. N. Khanna, *Science*, 2005, **307**, 231–235.
39 D. Y. Zubarev, B. B. Averkiev, H.-J. Zhai, L.-S. Wang and A. I. Boldyrev, *Phys. Chem. Chem. Phys.*, 2008, **10**, 257–267.
40 R. B. King, *Chem. Rev.*, 2001, **101**, 1119–1152.
41 Z. Chen and R. B. King, *Chem. Rev.*, 2005, **105**, 3613–3642.
42 P. M. Petrar, M. B. Sárosi and R. B. King, *J. Phys. Chem. Lett.*, 2012, **3**, 3335–3337.
43 A. I. Boldyrev and L.-S. Wang, *Chem. Rev.*, 2005, **105**, 3716–3757.
44 P. v. R. Schleyer, *Chem. Rev.*, 2001, **101**, 1115–1118.
45 C. Corminboeuf, C. S. Wannere, D. Roy, R. B. King and P. v. R. Schleyer, *Inorg. Chem.*, 2006, **45**, 214–219.
46 W. Fa and J. Dong, *J. Chem. Phys.*, 2006, **124**, 114310.
47 D. Tian and J. Zhao, *J. Phys. Chem. A*, 2008, **112**, 3141–3144.
48 B. Schaefer, R. Pal, N. S. Khetrapal, M. Amsler, A. Sadeghi, V. Blum, X. C. Zeng, S. Goedecker and L. Wang, *ACS Nano*, 2014, **8**, 7413–7422.
49 K. Joshi and S. Krishnamurty, *Phys. Chem. Chem. Phys.*, 2018, **20**, 8616–8623.
50 Y. Kondo and K. Takayanagi, *Science*, 2000, **289**, 606–608.
51 L. Cheng and J. Yang, *J. Chem. Phys.*, 2013, **138**, 141101.
52 L. Cheng, Y. Yuan, X. Zhang and J. Yang, *Angew. Chem., Int. Ed.*, 2013, **52**, 9035–9039.
53 L. Cheng, X. Zhang, B. Jin and J. Yang, *Nanoscale*, 2014, **6**, 12440–12444.
54 P. Jena and Q. Sun, *Chem. Rev.*, 2018, **118**, 5755–5870.
55 L. Cheng, C. Ren, X. Zhang and J. Yang, *Nanoscale*, 2013, **5**, 1475–1478.
56 L. Yan, L. Cheng and J. Yang, *J. Phys. Chem. C*, 2015, **119**, 23274–23278.
57 L. Liu, P. Li, L. Yuan, L. Cheng and J. Yang, *Nanoscale*, 2016, **8**, 12787–12792.
58 H. Wang and L. Cheng, *Nanoscale*, 2017, **9**, 13209–13213.
59 A. Munoz-Castro, *Chem. Sci.*, 2014, **5**, 4749–4754.
60 A. Muñoz-Castro, *ChemPhysChem*, 2016, **17**, 3204–3208.
61 A. Muñoz-Castro and R. B. King, *Int. J. Quantum Chem.*, 2017, **117**, e25331.
62 A. Muñoz-Castro and J.-Y. Saillard, *ChemPhysChem*, 2018, **19**, 1800–1800.
63 J. P. Perdew, K. Burke and M. Ernzerhof, *Phys. Rev. Lett.*, 1996, **77**, 3865–3868.
64 F. Weigend and R. Ahlrichs, *Phys. Chem. Chem. Phys.*, 2005, **7**, 3297–3305.
65 D. Y. Zubarev and A. I. Boldyrev, *Phys. Chem. Chem. Phys.*, 2008, **10**, 5207–5217.
66 X. Zhang, K. A. Lundell, J. K. Olson, K. H. Bowen and A. I. Boldyrev, *Chem. – Eur. J.*, 2018, **24**, 9200–9210.
67 M. J. Frisch, G. W. Trucks, H. B. Schlegel, G. E. Scuseria, M. A. Robb, G. Scalmani, V. Barone and D. J. Fox, *Revision B.01*, Gaussian, Inc., Wallingford CT, 2009.

68 U. Varetto, *MOLEKEL 5.0*, Swiss National Supercomputing Centre, Manno, Switzerland, 2009.
69 Q. Liu and L. Cheng, *J. Alloys Compd.*, 2019, **771**, 762–768.
70 Z. Tian and L. Cheng, *Phys. Chem. Chem. Phys.*, 2015, **17**, 13421–13428.
71 G. H. Kresse and J. Hafner, Ab initio molecular dynamics for liquid metals, *Phys. Rev. B: Condens. Matter Mater. Phys.*, 1993, **47**, 558.
72 J. P. Perdew, K. Burke and M. Ernzerhof, *Phys. Rev. Lett.*, 1996, **77**, 3865–3868.
73 G. J. Martyna, M. L. Klein and M. Tuckerman, *J. Chem. Phys.*, 1992, **97**, 2635–2643.
74 A. J. Bridgeman, G. Cavigliasso, L. R. Ireland and J. Rothery, *J. Chem. Soc., Dalton Trans.*, 2001, 2095–2108.
75 U. Ryde, R. A. Mata and S. Grimme, *Dalton Trans.*, 2011, **40**, 11176–11183.